

Available online at www.sciencedirect.com



Trans. Nonferrous Met. Soc. China 17(2007) 705-710

Transactions of Nonferrous Metals Society of China

www.csu.edu.cn/ysxb/

Effect of tube size on electromagnetic tube bulging

LI Zhong(李 忠), LI Chun-feng(李春峰), YU Hai-ping(于海平), ZHAO Zhi-heng(赵志衡) School of Materials Science and Engineering, Harbin Institute of Technology, Harbin 150001, China

Received 5 June 2006; accepted 16 April 2007

Abstract: The commercial finite code ANSYS was employed for the simulation of the electromagnetic tube bulging process. The finite element model and boundary conditions were thoroughly discussed. ANSYS/EMAG was used to model the time varying electromagnetic field in order to obtain the radial and axial magnetic pressure acting on the tube. The magnetic pressure was then used as boundary conditions to model the high velocity deformation of various length tube with ANSYS/LSDYNA. The time space distribution of magnetic pressure on various length tubes was presented. Effect of tube size on the distribution of radial magnetic pressure and axial magnetic pressure and high velocity deformation were discussed. According to the radial magnetic pressure ratio of tube end to tube center and corresponding dimensionless length ratio of tube to coil, the free electromagnetic tube bulging was studied in classification. The calculated results show good agreements with practice.

Key words: electromagnetic tube bulging; time varying electromagnetic field; magnetic pressure; high velocity deformation; dimensionless length

1 Introduction

Electromagnetic forming is one of high-energy-rate form technologies, using the Lorenz forces produced during discharge to form metal workpieces. The vehicle mass reduction is a major method to improve automotive fuel efficiency, and consequently, the use of aluminum alloys with low density and high strength is increased every year [1–10]. Electromagnetic forming of aluminum alloys provides improved forming limits, minimal springback and rapid implementation, thus electromagnetic forming has promising applications in auto industries.

LI et al[11] analysed the magnetic pressure acting on the tube with finite element method and the effects of length on the magnetic pressure of the tube were discussed. However, their calculated results were two-dimensional, the magnetic pressure was the average result in electromagnetic forming, and the effect of tube length on deformation was not considered. CALE code is used by FENTON and DAEHN[12] to calculate electromagnetic sheet forming, but the interactions among the electromagnetic field, thermal field, and structural field were ignored. BENDJIAMA et al[13]

proposed a coupling model to analyse dynamic plastic deformation of electromagnetic forming system. This model considered skin effect, eddy and motion of tube, but assumed that the generatrix remained straight in deformation, which was not consistent with practical situations. MERICHED et al[14] presented a model based on integral representation of magnetic vector potential to calculate the magnetic field, eddy, electromagnetic force density, but the effect of deformation velocity on magnetic field distribution and electromagnetic force was ignored.

Effect of tube thickness on electromagnetic tube bulging is very simple. When discharge current remains constant, magnetic pressure on the tube increases with the augment of tube thickness. However, forming velocity presents the reversed trend, and the details can be seen in Refs.[15–16]. The loose coupling method is used to analyse the electromagnetic tube bulging with different length in this study. ANSYS/EMAG is used to model the time varying electromagnetic field and far field element is used to mesh the region away from the forming coil in order to obtain the accurate solution of magnetic pressure under the condition of magnetic field diffusion. Magnetic pressure is then used as boundary conditions to model the high velocity deformation of

tube with ANSYS/LSDYNA. The effect of length on magnetic pressure and deformation is thoroughly considered, according to the radial magnetic pressure ratio of tube end to tube center and corresponding dimensionless tube length. The free electromagnetic tube bulging are studied in classification.

2 Transient electromagnetic field analysis

2.1 Model and boundary conditions

Because the axially symmetrical characteristics of electromagnetic tube bulging, only the half of forming system needs to be considered. The finite element model is shown in Fig.1, where A1, A2 refer to the coil and tube respectively, A3 is air far field region, A4 is air near field region, h equals the half of the coil length. Fig.2 shows the mesh of magnetic field FEM model. To avoid the calculation complexity of energy transformation, discharge current is used as the excitation in the present analysis. This treatment can be closer to the practical situation during forming process. The discharge current wave is shown in Fig.3. The materials properties of the forming system are listed in Table 1. According to Ref.[2], boundary conditions are built as follows. 1) In

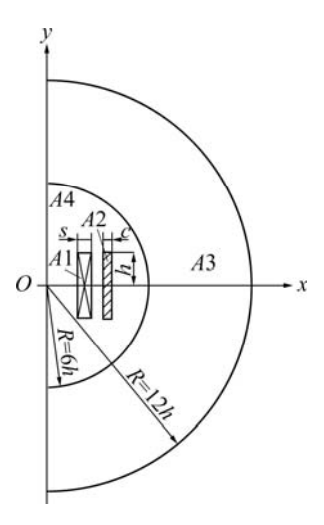


Fig.1 FEM analysis model of magnetic field in electromagnetic tube bulging

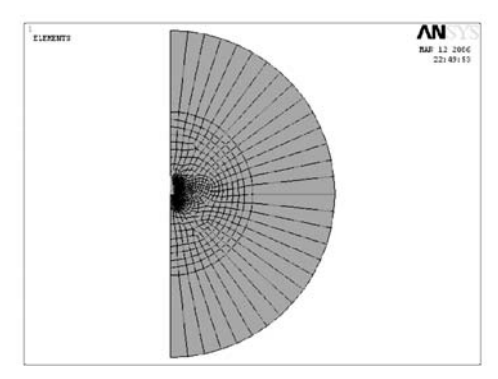


Fig.2 Mesh of magnetic field FEM analysis

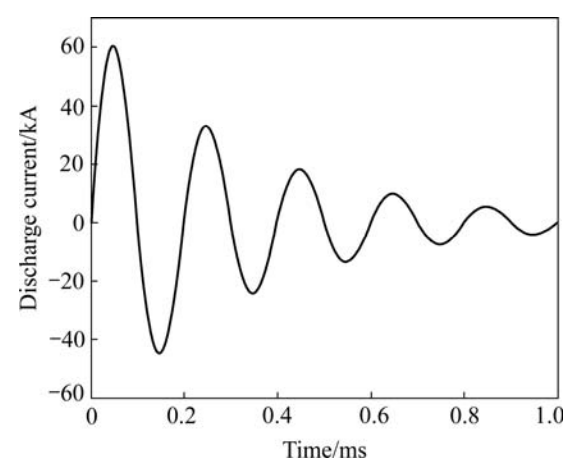


Fig.3 Relations of discharge current and time

Table 1 Parameters of forming system

Material	Property	Value	
Free region (air)	Relative permeability	1	
Coil wire (Cu)	Relative permeability	1	
	Resistivity/(Ω ·m)	1.724×10^{-8}	
	Gap/mm	1.0	
	Turns	22	
	Length/mm	100	
Tube (3A21)	Relative permeability	1	
	Resistivity/ $(\Omega \cdot m)$	3.346×10^{-8}	
	Thickness/mm	1.2	
	Length	Self-defined	

the Cartesian coordinate system, B (magnetic induction intensity) at Y=0 is perpendicular to X axis. 2) In the Cartesian coordinate system, A (magnetic potential vector) at X=0 equals to zero. 3) In the polar coordinate system, an infinite flag is set at $\rho=12h$.

2.2 Results and discussion

Time space distributions of magnetic pressure in the cases of 60, 100 and 140 mm in length are shown in Figs.4–6 respectively (the origin is at the tube length center, the positive direction of axial magnetic pressure is upward, and the positive direction of radial magnetic pressure is towards the outer normal of tube). Axial magnetic pressure is greater at tube end and less in the region far away from the end. The axial magnetic pressure at the center is zero in the cases of 60, 100 and 140 mm in length; axial magnetic pressure is greater at the location equal to the coil length and decreases to the adjacent region. This distribution characteristic of axial magnetic pressure is determined by the distributions of magnetic flux lines.

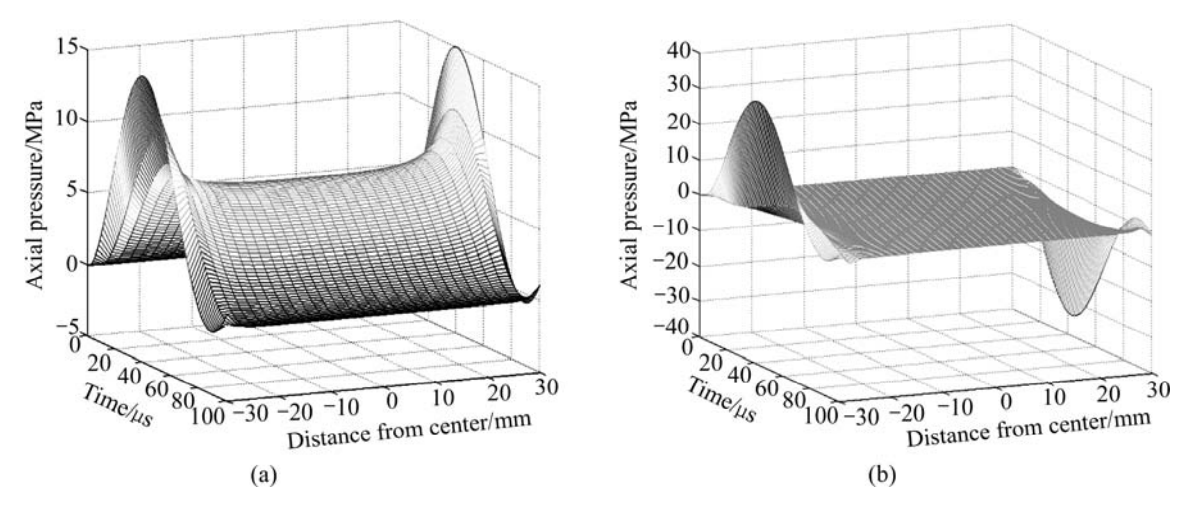


Fig.4 Distribution of magnetic pressure of 60 mm-long tube: (a) Radial magnetic pressure; (b) Axial magnetic pressure

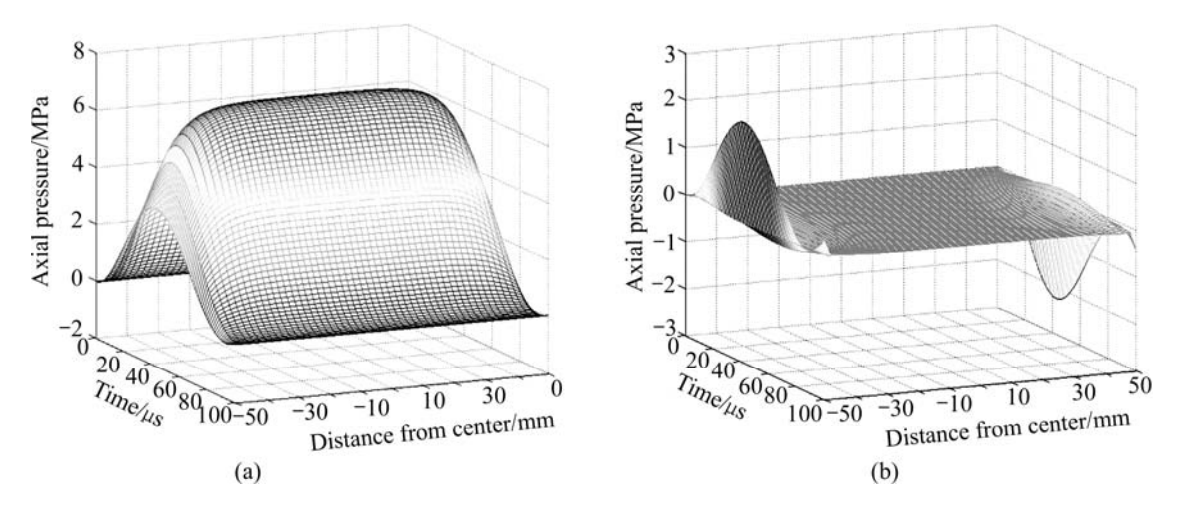


Fig.5 Distribution of magnetic pressure of 100 mm-long tube: (a) Radial magnetic pressure; (b) Axial magnetic pressure

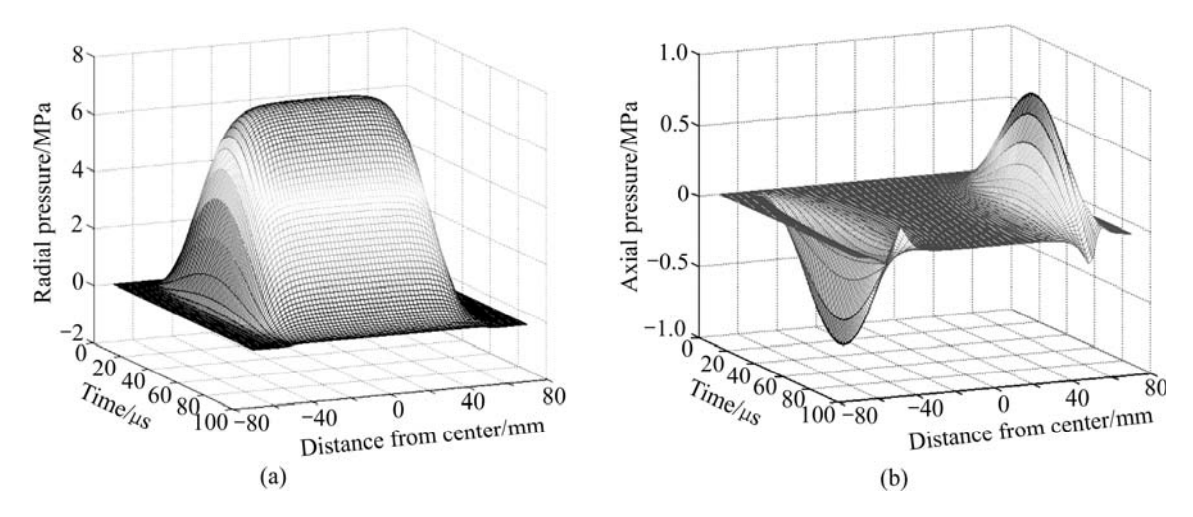


Fig.6 Distribution of magnetic pressure of 140 mm-long tube: (a) Radial magnetic pressure; (b) Axial magnetic pressure

Magnetic flux lines are not parallel to the tube wall at the tube end in the cases of 60 and 100 mm in length, and there is greater radial component of magnetic induction intensity, so the axial magnetic pressure is greater there. But in the other region, the radial

component of magnetic induction intensity is little, as a result, the axial magnetic pressure there is slight. The distribution of axial magnetic pressure of 140 mm-long tube can be explained in the same way. The radial magnetic pressure decreases gradually from the tube end

to the center of tube length in the case of 60 mm in length, but increases in the cases of 100 and 140 mm in length. The radial magnetic pressure difference between the tube end and the tube center is greater, so a function is defined as follows in order to represent the non-uniformity:

$$R(t,L) = \frac{p_{\rm e}}{p_{\rm c}} \tag{1}$$

where $p_{\rm e}$ is the radial magnetic pressure at the tube end, and p_c refers to the radial pressure at the tube center. The function is plotted in Fig.7. As shown in the curves, the ratio is close to zero in the case of 140 mm in length; and the ratio is less than 1 and decreases with time. As time approaches 100 µs, the ratio increases unconventionally in the case of 100 mm in length. This is because the cycle of magnetic pressure at end is little less than that at the center. When the time approaches 100 µs, radial magnetic pressure at the center is slight, but the radial magnetic pressure at the end enters into the next cycles in advance. In the case of 60 mm in length, the ratio basically is greater than 1, and its evolution with time is the same as the case of 100 mm in length. Because the ratio function varies with time and tube length, the values of the function at discharge current's peak, R, is selected to represent the average non-uniformity, as shown in solid lines in Fig.8, where *l* is dimensionless length defined by the length ratio of tube to coil. When R is greater than 1, the greater the R value is, the more uneven the radial magnetic pressure distribution is. When R is less than 1, the smaller the R value is, the more uneven the radial magnetic pressure distribution is. As shown in Fig. 8, on the right of point A, the ratio R is less than 1, and approaches zero with the increase of length. On the left of point A, the ratio R is greater than 1, and increases with the decrease of length first, then decreases gradually. At the critical point A, the ratio R is equal to 1, radial magnetic pressure is distributed uniformly, and dimensionless length l here is approximately

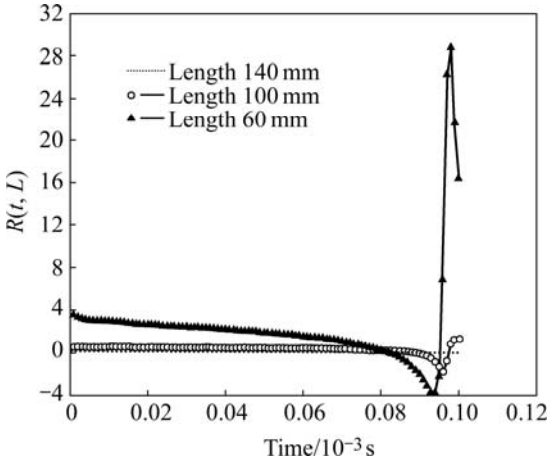


Fig.7 Function curves of R(t, L)

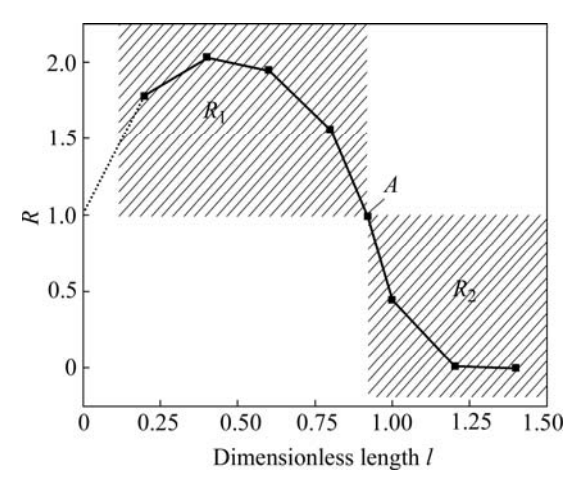


Fig.8 Relations of R and dimensionless length l

0.92. We extend the solid lines to zero as shown in dash line in the graph, and the ratio approaches 1, i.e., as the length is zero, the distribution of radial magnetic pressure gets more uniform. The correlative proofs can be found in Ref.[3]. The radial magnetic pressure at the end is greater than that at the center in the shadow region R_1 and the situation in the shadow region R_2 is quite reverse.

3 Transient structural analysis

The mechanical properties of material chosen in this analysis are listed in Table 2. The simulation graph of deformed aluminum tubes are shown in Fig.9. The deformation at the tube end is greater than that at the center in the cases of 60 and 80 mm in length, because their dimensionless length lies in the R_1 region of Fig.8, where the radial magnetic pressure decreases from the tube end to the tube center. The deformation at the tube end is less than that at the center in the cases of 100 and 140 mm in length, as their dimensionless length locates in the R_2 region, where the radial magnetic pressure distributions are reverse to the cases of 60 and 80 mm in length. Dimensionless length of 92 mm-long tube is 0.92, and its location in Fig.8 is at the critical point A, where the distribution of radial magnetic pressure is more uniform, as a result, the deformation remains almost the same along the tube length. The relations of radial displacement and time in the cases of 80, 92 and 140 mm in length are shown in Figs. 10-12, respectively. The radial displacement at the end is greater than that at the center all the time, as shown in Fig.10. As the radial magnetic pressure at the end is greater, the deformation at the end continues to increase, but the deformation at the center is slight when the time is 100 us, the deformation along the tube finishes when the time is 150 μs. Because the radial magnetic pressure is distributed more uniformly, the radial displacement remains almost

Table 2 Mechanic properties of material

Material	Elastic modulus, E/MPa	Yield stress, σ_0 /MPa	Strain hardening coefficient, n	Strength coefficient, <i>K</i> /MPa
3A21	68 400	44	0.227	330.2

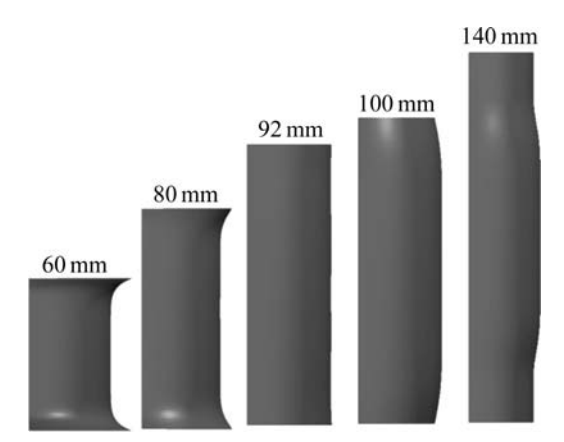


Fig.9 Simulation graphs of deformed aluminum tubes with various lengths

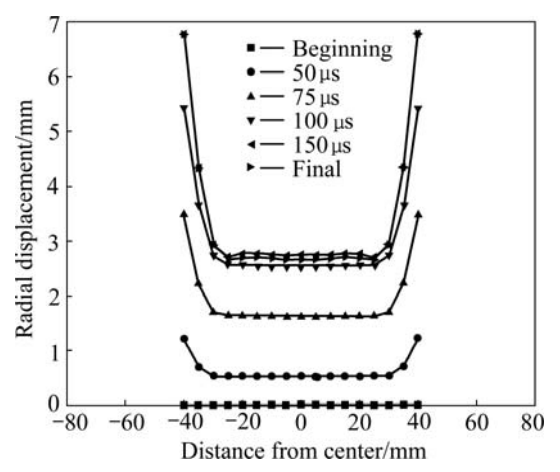


Fig.10 Relations of radial displacement and time of 80 mm-long tube

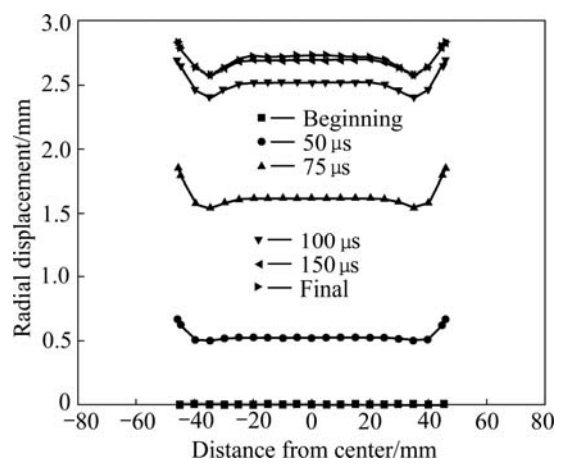


Fig.11 Relations of radial displacement and time of 92 mmlong tube

uniform in the case of 92 mm in length during the bluging. The maximum value of the radial displacement difference is 0.25 mm, compared with the final radial displacement of 2.83 mm. The maximum relative difference is 8.8%, and the generatrix of the tube remains almost straight during the whole forming process. The radial displacement at the end is zero, as shown in Fig.12, because the radial pressure at the end is far less than that at the center. When the time is 100 µs, the deformation of location equal to the coil length is finished basically, but the tube center continues to deform. The deformation along the whole tube finishes at the time of 150 µs. As shown in Fig.13, the first principal strain varies from 0.10 to 0.11, and the thickness varies from 1.10 to 1.12 mm. They are distributed more uniformly in the case of 92 mm in length. This is also the results of uniform distribution of radial magnetic pressure. The deformed workpieces is shown in Fig.14. It can be seen that the calculated results show good agreements with practices.

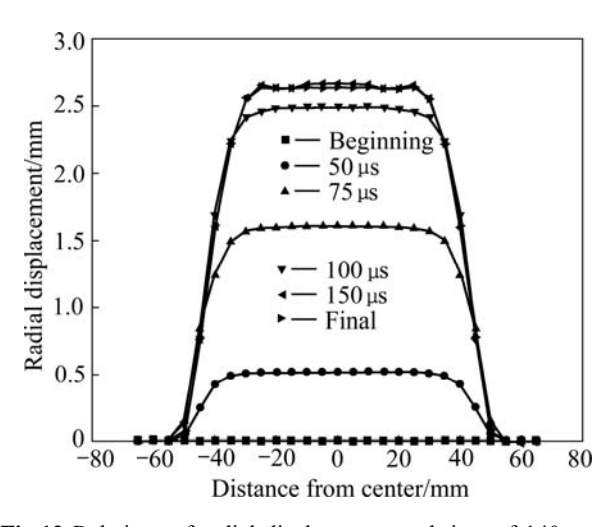


Fig.12 Relations of radial displacement and time of 140 mm-long tube

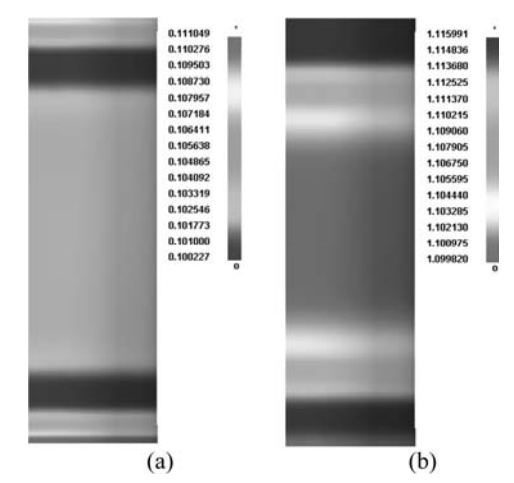


Fig.13 Distribution of first major strain and thickness of 92 mm-long tube after deformation: (a) First principal strain; (b) Thickness

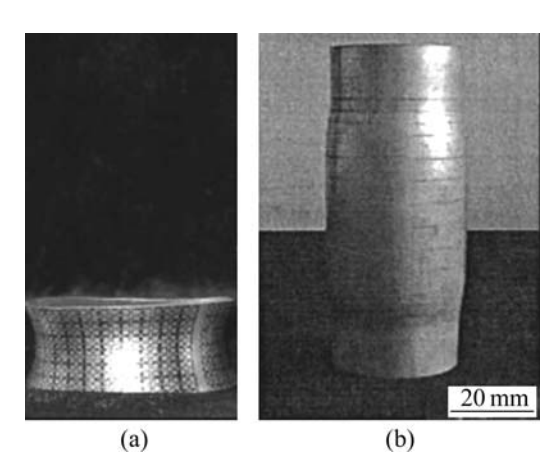


Fig.14 Deformed workpieces: (a) Length of 30 mm; (b) Length of 140 mm[11]

4 Conclusions

- 1) The time space distribution of magnetic pressure is given. This is very beneficial to understanding the mechanism of electromagnetic forming and promoting engineering applications of electromagnetic forming.
- 2) When the tube length is smaller or equal to the coil length, axial magnetic pressure is greater at the end. When the tube length is bigger than the coil length, axial magnetic pressure is greater at the location equal to the coil length and decreases to the adjacent region. At the center, axial magnetic pressure of various sizes of tube is zero.
- 3) When the dimensionless tube length is less than 0.92, the radial magnetic pressure at the end is greater than that at the center. The non-uniformity extent of radial magnetic pressure increases with the decrease of dimensionless length first, and then decreases gradually. As the dimensionless length approaches zero, radial magnetic pressure tends to be distributed uniformly. When the dimensionless tube length is the bigger than 0.92, the radial pressure at the end is less than that at the center. The non-uniformity extent of radial magnetic pressure increases with dimensionless length first, then tends to be steady. When the dimensionless tube length is equal to 0.92, the radial magnetic pressure is distributed more uniformly.
- 4) When the dimensionless tube length lies in R_1 region, deformation along the tube is uneven, and deformation of tube end is greater than that of tube center. When the dimensionless tube length is in the R_2 region, the deformation along the tube is also uneven, and the deformation of tube end is less than that of tube center.

When the dimensionless tube length approaches 0.92 and 0, the tube tends to be formed uniformly. The calculated results show good agreements with experimental results.

References

- PARK Y B, KIM H Y, OH S I. Design of axial/torque joint made by electromagnetic forming [J]. Thin-Walled Structure, 2005, 43: 828–844.
- [2] LEE S H, LEE D N. Estimation of magnetic pressure in tube expansion by electromagnetic forming [J]. Journal of Materials Processing Technology, 1996, 57: 311–315.
- [3] TAMHANE A A, ALTYNOVA M M, DAEHN G S. Effect of sample size on ductility in electromagnetic ring expansion [J]. Scripta Materialia, 1996, 34:1345–1350.
- [4] AZAB A E, GARNICH M, KAPOOR A. Modeling of the electromagnetic forming of sheet metals: State-of-the-art and future needs [J]. Journal of Materials Processing Technology, 2003, 142: 744-754.
- [5] BEDNARCZYK J. Distributions of forces in the inductors used in metal processing in the pulse magnetic field [J]. Journal of Materials Processing Technology, 2003, 133: 340–347.
- [6] MAMALIS A G, MANOLAKOS D E, KLADAS A G, KOUMOUTSOS A K. Physical principles of electromagnetic forming process: A constitutive finite element model [J]. Journal of Materials Processing Technology, 2005, 161: 294–299.
- [7] SETH M, VOHNOUT V J, DAEHN G S. Formability of steel sheet in high velocity impact [J]. Journal of Materials Processing Technology, 2005, 168: 390–400.
- [8] GIANNOGLOU A, KLADAS A, TEGOPOULOUS J. Electromagnetic forming: A coupled numerical electromagneticmechanical-electrical approach compared to measurements [J]. International Journal for Computation and Mathematics in Electrical and Electronic Engineering, 2004, 23(3): 789–799.
- [9] OLIVEIRA D A, WORSWICK M J. Electromagnetic forming of aluminum alloy sheet [J]. J Phys IV, 2003, 110: 293–298.
- [10] OLIVEIRA D A, WORSWICK M J. Simulation of electromagnetic forming of aluminum alloy sheet [J]. SAE Trans J Mat Manuf, 2001, 110: 687–695.
- [11] LI Chun-feng, ZHAO Zhi-heng, LI Jian-hui, LI Zhong. The effect of tube length on magnetic pressure in tube electromagnetic bulging [J]. Journal of Materials Processing Technology, 2005, 166: 381–386.
- [12] FENTON G K, DAEHN G S. Modeling of electromagnetically formed sheet metal [J]. Journal of Materials Processing Technology, 1998, 75: 6–16.
- [13] BENDJIMA B, SRAIRI K, FÈLIACHI M. A coupling model for analyzing dynamical behaviors of an electromagnetic forming system [J]. IEEE Transactions on Magnetics, 1997, 33(2): 1638–1641.
- [14] MERICHED A, FÈLIACHI M, MOHELLEBI H. Electromagnetic forming of thin metal sheets [J]. IEEE Transactions on Magnetics, 2000, 36(4): 1808–1811.
- [15] LI Zhong. Research on electromagnetic tube bulging and forming limit under electromagnetic forming [D]. Harbin: Harbin Institute of Technology, 2007.
- [16] ZHAO Zhi-heng. Study on magnetic pressure in tube electromagnetic bulging [D]. Harbin: Harbin Institute of Technology, 2001.

(Edited by YANG Bing)